Abridged version

KAWASAKI STEEL TECHNICAL REPORT
No.28 (June 1993)
Special Issue on Chemicals and
New Materials and Construction Materials

Deformation Behavior of Metal Injection-Molded Compacts During Sintering

Keiichi Maruta, Yukio Makiishi, Hiroshi Ohtsubo, Shigeaki Takajo

Synopsis :
The shape deformation behavior during sintering was measured and correlated to the bonding between particles in injection-molded compacts. Stainless steel powders of different particle size were injection melded and sintered. Sintering shrinkage began at around 1000℃, and a finer powder promoted sintering. Before sintering shrinkage occurred, residual carbon from the binder was concentrated on the particle surface and contributed to the adherence between particles in a compact. This carbon decreased as a result of the C-O reaction up to 1000℃. Therefore, the bonding between particles loosened transiently, and shape deformation of the compact occurred during this stage. The promotion of sintering by means of fine powder suppressed this shape deformation. The shape deformation behavior during sintering was simulated by the finite element method, and the result is in good agreement with the experimental results.

The body can be viewed from the next page.

Deformation Behavior of Metal Injection-Molded Compacts During Sintering*


Keiichi Maruta
New Materials Dept.,
Chemical Div.


Yukio Makiishi
New Materials Dept.,
Chemical Div.


Hiroshi Ohtsubo
Manager,
New Materials Dept.,
Chemical Div.


Shigeaki Takajo
Dr. Sci. & Dr. Eng.,
Senior Researcher,
New Materials Research
Center, High-
Technology Res. Labs.

Synopsis:

The shape deformation behavior during sintering was measured and correlated to the bonding between particles in injection-molded compacts. Stainless steel powders of different particle size were injection molded and sintered. Sintering shrinkage began at around 1 000°C, and a finer powder promoted sintering. Before sintering shrinkage occurred, residual carbon from the binder was concentrated on the particle surface and contributed to the adherence between particles in a compact. This carbon decreased as a result of the C–O reaction up to 1 000°C. Therefore, the bonding between particles loosened transiently, and shape deformation of the compact occurred during this stage. The promotion of sintering by means of fine powder suppressed this shape deformation. The shape deformation behavior during sintering was simulated by the finite element method, and the result is in good agreement with the experimental results.

1 Introduction

Metal injection molding (MIM) is a new process in which fine metal powder with a mean diameter of about 10 μm is mixed with an organic binder, injection molded, the binder removed, and the molded body sintered. While only two-dimensional shapes can be made by press compaction, MIM is suited for mass producing complex shapes.[1,2] The fine powder enables the relative density of the sintered compact to attain over 95%, which can't be achieved by press compaction.[3,4] MIM is particularly favorable for the corrosion resistance of sintered stainless steel because of the high density.[5]

The shape of the green compact is held by a binder, and therefore, the debound compact is very fragile. A compact often chips and loses its shape before sintering. While the sintered density is very high, the shrinkage is 15–20%, so that it is difficult to keep dimensional precision. The shape of the compact also deforms substantially during sintering; for example, deformation like bending or buckling occurs due to gravity, and friction between a compact and the support tray often deforms the shape.

This shrinkage between a green compact and the sintered product must be considered when designing the molding die, and methods for predicting the deformation are also required. The finite element method (FEM) has been studied for analyzing the deformation of ceramic compacts,[6,7] and the prediction and control of dimensional precision have also been researched.[8,9]

The bonding between particles in injection-molded compacts was investigated by using 316L water-atomized powders of different particle size. The deformation behavior of rectangular specimens supported at their ends and of cup specimens was measured and correlated with the bonding between particles. Suppression of this deformation by using fine powders was investigated, the deformation being simulated by FEM.

* Originally published in *Kawasaki Steel Giho*, 24(1992)2, 129–134

2 Shrinkage of Metal Injection Molded Compacts during Sintering

2.1 Experimental Methods

316L stainless steel powders produced by water atomization were used, **Table 1** showing the composition of these powders. Each powder was sieved to three particle sizes to evaluate the relationship between the particle size and sintering shrinkage. **Table 2** shows the powder size distribution, powder A being the finest with powders B and C next in particle size.

These powders were mixed with an organic binder and injection molded into rectangular specimens (11.9 mm × 65.5 mm × 5.95 mm). The powder packing density was a constant 60 vol%.

The compacts were debound in a nitrogen atmosphere at 650°C, and then sintered in a vacuum at 1 350°C for 2 h. Powder particles of compacts sintered at 900, 1 000, and 1 100°C were observed by a scanning electron microscope. The sintered density was measured by the water method, the full density of SUS316L being 7.99 g/cm^3. The shrinkage during sintering was investigated by a dilatometer, and the surface of particles in the compacts was investigated during the course of sintering by Auger electron spectroscopy.

To estimate the deformation behavior, specmens supported at their ends over a span of 50 mm were sintered, and the amount of deformation at the center was measured. Cast specimens with the same chemical composition as the compacts were also measured by the same test method for comparison. The model used for simulating deformation by an FEM analysis was a cup specimen. A cup specimen is easy for analyzing the deformation and coordinating with actual parts. Cup specimens with an external diameter of 30 mm, internal diameter of 26 mm, and height of 20 mm were injection molded by using powder C, and the height and the side profile of each sintered cup specimen were measured and compared with the results calculated by FEM.

Table 1 Chemical composition of water atomized powder used for experiments (wt %)

C	Si	Mn	Ni	Cr	Mo	O
0.02	0.75	0.40	15.2	18.4	3.5	0.65

Table 2 Size distribution of powders used for experiment (μm)

Powder	D_{10}[a)]	D_{50}[b)]	D_{90}[c)]	M_v[d)]
A	2.56	6.28	19.41	8.86
B	3.72	8.90	19.04	10.51
C	4.42	10.26	23.67	12.31

a) D_{10}: Diameter at 10% accumulative weight
b) D_{50}: Diameter at 50% accumulative weight
c) D_{90}: Diameter at 90% accumulative weight
d) M_v: Volume mean diameter

2.2 Results and Discussion

2.2.1 Shrinkage during sintering

The relationship between the densification during sintering and powder size was investigated. **Figure 1** shows the sintered density as a function of temperature. Sintering densification began at around 1 000°C, and the sintered density increased rapidly between 1 000°C and 1 100°C. At 1 100°C, the relative density of powder A, which was the finest, was 3% more than that of powder C, which was the coarsest. A relative density of over 95% was attained.

Photo 1 shows the microstructure of a sintered compact made from powder C. The porosity is fine and even, and this sintered compact had sufficient corrosion resistance.[10]

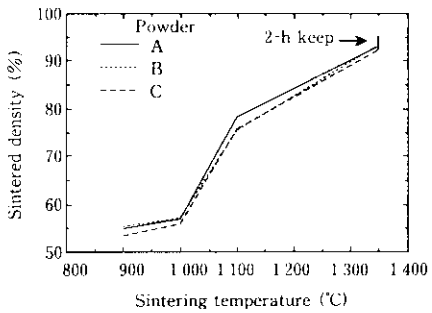

Fig. 1 The change of sintered density as a function of sintering temperature

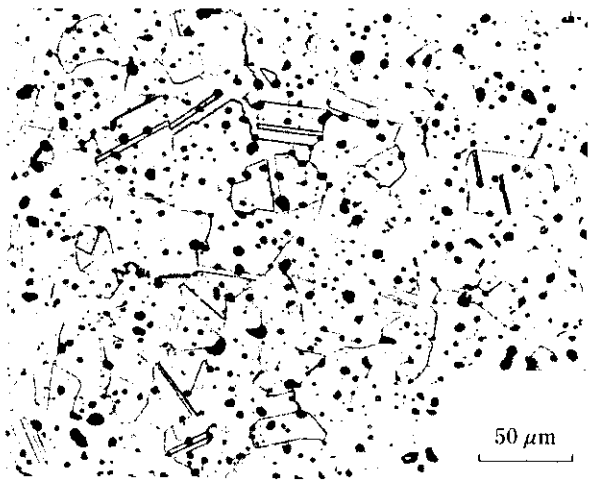

Photo 1 Microstructure of sintered compact made from powder C

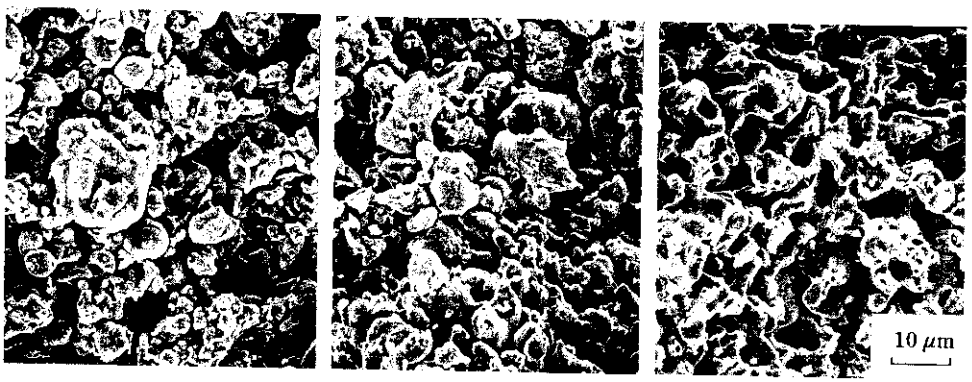

900°C　　1 000°C　　1 100°C

Photo 2 Change in contact condition of compacts sintered at 900, 1 000 and 1 100°C

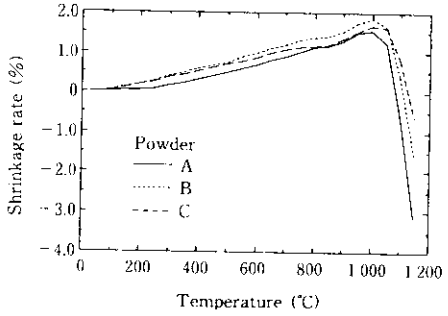

Fig. 2 The shrinkage rates of compacts made from powders A, B and C as a function of temperature

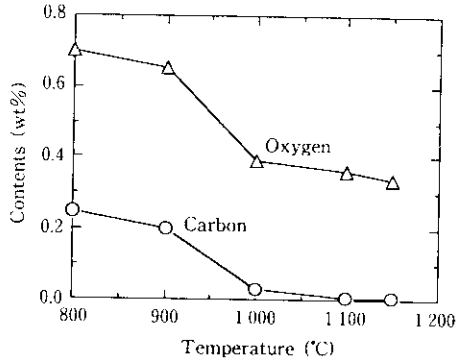

Fig. 3 The contents of carbon and oxygen as a function of temperature

Figure 2 shows the shrinkage of the compacts, which was measured by a dilatometer, as a function of temperature. Sintering shrinkage began at around 1 000°C and progressed rapidly. Finer powder promoted finer sintering, the shrinkage of powder A being 2% more than that of powder C at 1 100°C.

The cross sections of compacts sintered at 900°C, 1 000°C and 1 100°C were investigated by SEM in order to observe the change of bonding between particles, **Photo 2** showing the SEM photographs. The particles were only touching each other at 900°C. At 1 000°C, the fine particles became bonded to large particles, but no neck growth due to sintering was apparent. As sintering progressed further to 1 100°C, and the shape of discrete particles disappeared.

Initially, the particle of an injection-molded compact were bound by an organic binder. After debinding, the residual carbon or oxygen on the particle surface will affect sintering. **Figure 3** shows the contents of carbon and oxygen in compacts made from powder C as a function of temperature. The content of carbon was 0.25% up to 800°C, above which carbon and oxygen began to decrease at around 900°C. **Figure 4** shows the results by thermogravimetry of debound compacts during sintering in a vacuum. The weight of the debound compacts began to decrease at 900°C. The residual carbon and oxygen were removed as a result of the C–O reaction, which progressed from around 900°C, carbon being almost lost at 1 000°C. The final carbon content was 0.003%, and this loss of carbon during sintering is

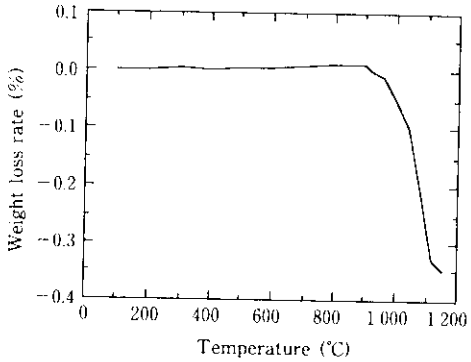

Fig. 4 The results of thermogravimetry of debinded compacts during sintering in vacuum

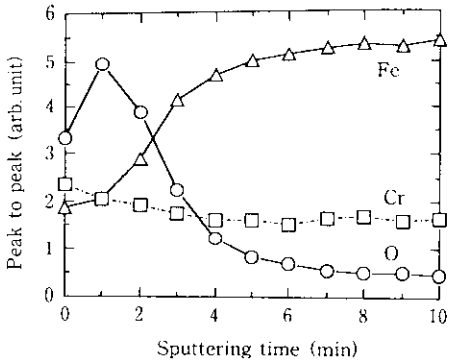

Fig. 5 Auger depth profiles of Fe, Cr and O for water atomized powders of SUS316L

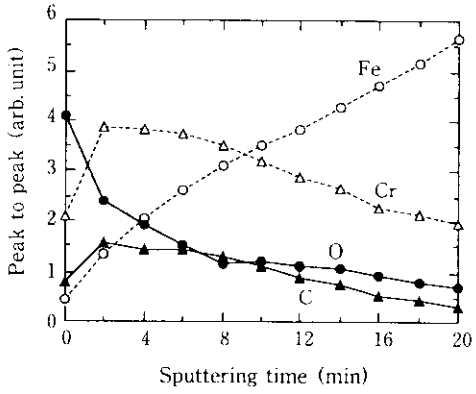

Fig. 6 Auger depth profiles of Fe, Cr, O and C in a compact sintered at 900°C

important for the corrosion resistance of stainless steel.[10]

Figure 5 shows Auger depth profiles for water-atomized powder of SUS316L. The oxygen content was 0.65% in the powder, and oxygen was concentrated at the surface of the particles.

Figures 6 and 7 show Auger depth profiles for the powder in compacts respectively sintered at 900°C and 1 000°C as shown in Photo 2. Carbon was concentrated at the surface of the particles at 900°C in similar way to oxygen, but had almost disappeared in the compact sintered at 1 000°C.

Carbon and oxygen concentrated at the particle surface began to decrease at around 900°C. At 1 000°C, the carbon had almost disappeared, and sintering shrinkage began at this stage. The electricity, the van der Waals attraction and the residual binder between particles contribute to the connection between particles of a debound compact.[11] Consequently, the residual carbon concentrated at the interface between particles in the compacts contributed to the connection between particles, and caused the bonding to weaken transiently just before 1 000°C. Sintering shrinkage then progressed

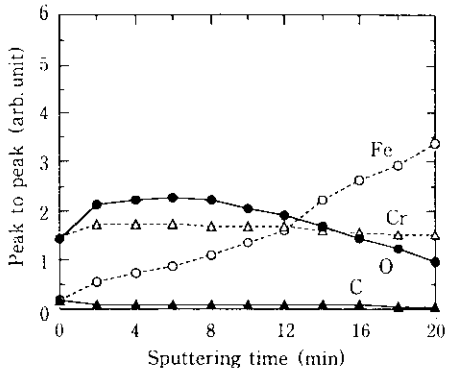

Fig. 7 Auger depth profiles of Fe, Cr, O and C in a compact sintered at 1 000°C

rapidly between 1 000°C and 1 100°C, the particle size having an effect on sintering during this stage, sintering progressing more rapidly with decreasing particle size.

2.2.2 Deformation behavior during sintering

Figure 8 shows the deformation of specimens supported at their ends during sintering. The deformation did not progress much up to 1 000°C, then increased rapidly between 1 000°C and 1 100°C, and remained fairly constant at above 1 100°C. Powder size had an effect on this deformation. The deformation of sintered compacts made from powders A and B, which were finer, was smaller than that of powder C, the final deformation of sintered compacts made from powder A being almost 50% that of powder C compacts.

Gravity caused this deformation. The cast specimen with the same chemical composition as that of the sintered compacts did not deform with heating as shown in Fig. 8, so that the densification due to sintering had an effect on this deformation.

Carbon and oxygen, which were concentrated at the interface between particles, decreased at just below 1 000°C, although sintering had not progressed at that

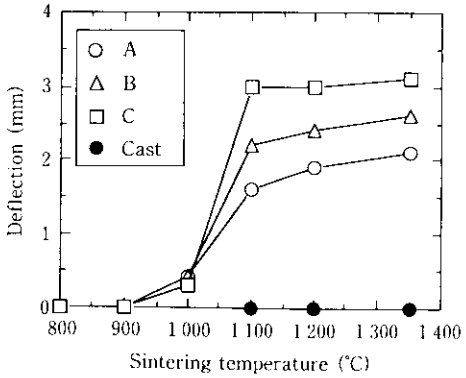

Fig. 8 The deflection of compacts made from powders A, B and C, comparing casting specimen during sintering

temperature. Therefore, the bond between particles loosened and deformation progressed rapidly at that stage. Above 1 100°C, sintering had progressed, and the skeletal structure formed is shown in Photo 2. Further deformation was suppressed due to this structure. Fine powder promoted sintering shrinkage above 1 000°C and suppressed this deflection.

Figure 9 shows the difference in dimensional change between the height at the center and corner, and between the diameter at the top and bottom of the cup specimen. Difference $H_e - H_c$ shows the height at the corner minus the height at the center, while difference $D_b - D_t$ shows the effect of constraint by the bottom. These differences in dimensional change increased rapidly just above 1 000°C. The difference in dimensional change between the diameter at the top and bottom was 0.35 mm for a cup specimen whose height was 20 mm.

Figure 10 shows the side profile of the sintered cup measured by a coordinate measuring machine, indicating that the bottom of the cup spread during sintering. This spread was not detected in the green compacts, and therefore, the deformation occurred during sintering.

Although the deformation of a simple cup shape was investigated, the deformation behavior during sintering

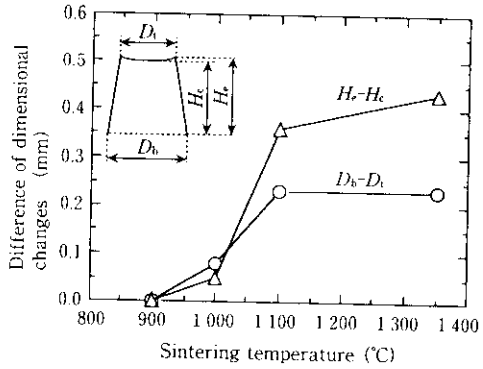

Fig. 9 Inhomogeneous shrinkage of diameter and height during sintering (Specimen: cup)

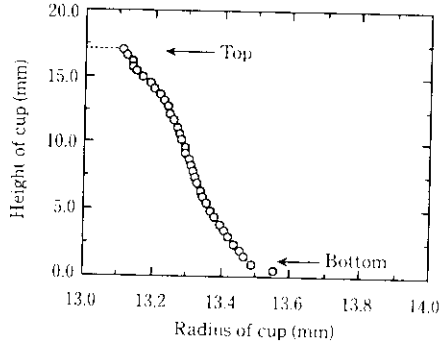

Fig. 10 The side profile of sintered cup compacts

varies according to the shape. The manufacture of complex shapes is an objective of metal injection molding, so that predicting and controlling the deformation is important. In the next section, the simulation of deformation during sintering will be investigated.

3 Simulation of Deformation during Sintering

3.1 Basic Theory

In this report, sintered compacts was assumed to be continuity, and the finite element method was applied to analyze the deformation. The program used for this simulation was developed according to the formula proposed by Dr. Yamada.[12,13] The degree of bonding between particles increases because of neck growth during sintering, and decreases because of the reduction in strength at the neck according to temperature. In this simulation, the deformation caused by force working on the particles is assumed to be that by creep. The strain occurring during sintering can be represented by

$$\{\dot{\varepsilon}\} = \{\dot{\varepsilon}_e\} + \{\dot{\varepsilon}_p\} + \{\dot{\varepsilon}_c\} + \{\dot{\varepsilon}_\alpha\} \quad \cdots\cdots\cdots\cdots (1)$$

where $\{\dot{\varepsilon}_e\}$ expresses the elastic strain, $\{\dot{\varepsilon}_p\}$ expresses the plastic strain, and $\{\dot{\varepsilon}_\alpha\}$ expresses the strain due to sintering shrinkage. Creep strain $\{\dot{\varepsilon}_c\}$ is a function of stress, temperature, time and sintered density. The change in $\{\dot{\varepsilon}_c\}$ from the results of specimens supported at their ends shown in the foregoing section was applied to this simulation.

From the results shown in Fig. 8, strain ε was calculated from the amount of deformation, and stress σ was calculated from the specimen size and sintered density. The following equation was then obtained:

$$|\dot{\varepsilon}_c| = 1.627 \times 10^{-7} \sigma^{0.44} t^{0.5} (-T + 950)(T - 1170) \quad \cdots\cdots\cdots\cdots (2)$$

where t is the sintering time, and T is the sintering temperature.

The strain due to sintering shrinkage, $\{\dot{\varepsilon}_\alpha\}$, can be treated similarly to heat expansion strain. Shrinkage coefficient α at each temperature was obtained from the curve shown in Fig. 2, and shrinkage strain $\{\dot{\varepsilon}\}$ was then calculated as

$$\{\dot{\varepsilon}\} = [\alpha \Delta T,\ \alpha \Delta T,\ \alpha \Delta T, 0, 0, 0] \quad \cdots\cdots\cdots\cdots (3)$$

3.2 Results of the Simulation

According to the assumptions expressed by basic theory, the deformation of the sintered cup was simulated under the same conditions as those used in the experiment. **Figure 11** shows the model used for the simulation, the initial condition being at 950°C just before sintering shrinkage, and the heating rate being 10°C/min. In this simulation, plastic strain was assumed to be involved in the creep strain. Young's modulus was 7.51×10^{10} Pa, and Poisson's ratio was 0.3. This value

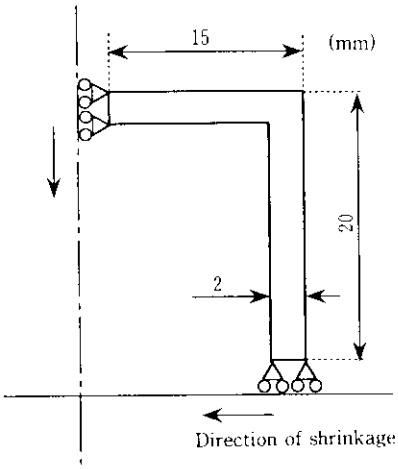

Fig. 11 The cup model used for simulation

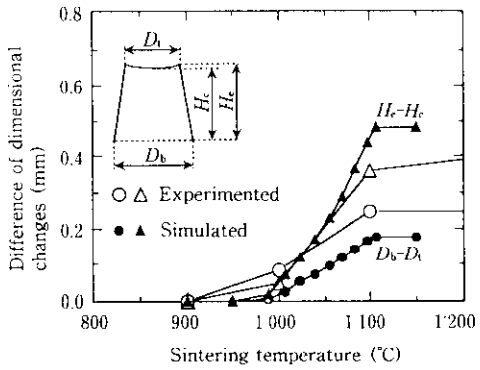

Fig. 12 The results of simulation for inhomogeneous shrinkage

for Young's modulus is that for austenitic stainless steel at 950°C, which is constant regardless of the density and temperature. The number of elements was 400 and the number of nodes was 255.

Figure 12 compares the result of the simulation with the experimental results, in which the base of the cup was deformed inwards and the lip expanded. Deformation progressed rapidly at around 1 000°C, the calculated figures being in good agreement with the experimental results.

This proves the suitability of the finite element method to simulate the deformation during sintering, and this simulation should be able to handle other shapes of compact.

4 Conclusions

The sintering shrinkage and deformation behavior of metal injection-molded compacts made from stainless steel powders were investigated.

(1) Sintering shrinkage progressed rapidly up to 1 000°C and was promoted by the fineness of powder.
(2) Residual carbon from the organic binder was concentrated on the surface of the powder and contributed to the bond between powder particles.
(3) This residual carbon decreased before sintering shrinkage as a result of the C–O reaction. Therefore, the bond between particles loosened transiently and deformation of the compacts progressed rapidly up to 1 000°C.
(4) Fine powder promoted sintering and suppressed this shape deformation.
(5) It was possible to simulate the deformation behavior during sintering by using the finite element method.

References

1) R. Billiet: *Int. J. Powder Met. Powder Tech.*, **21**(1985), 119
2) L. F. Peace III: *Int. J. Powder Met. Powder Tech.*, **22**(1986), 117
3) Y. Kiyota and H. Ohtsubo: *Funtai oyobi Funmatsu Yakin (J. Jpn. Soc. Powder and Powder Metall.)*, **5**(1990)37, 601
4) H. Zhang, R. M. German, K. F. Hens, and D. Lee: *Powder Metall. Int.*, **22**(1990)6, 15
5) S. Takajo: *Kinzoku (Metals & Technology)*, **2**(1991), 35
6) K. Mori, K. Osakada, and T. Hirano: "Hot Isostatic Pressing-Theory and Applications", ed. M. Koizumi, (1991), 29, [Elsevier Applied Science]
7) K. Mori, K. Osakada, T. Yoneda, and T. Hirano: *Sosei to Kako (J. Jpn. Soc. Tech. Plasticity)*, *32*(1991)368, 1136
8) F. Vollertsen and M. Geiger: *Powder Metall. Int.*, **22**(1990)3, 15
9) K. F. Hens, D. Lee, S. T. Lin, and R. M. German: *Powder Metall. Int.*, **23**(1991)1, 15
10) Y. Kiyota, H. Ohtsubo, I. Sakurada, J. Ohta, and S. Takajo: *Advances in Powder Metallurgy*, **3**(1990), 455
11) R. M. German: "Powder Injection Molding", 301, [Metal Powder Industries Federation]
12) Y. Yamada, T. Hirakawa, and A. S. Will: Proceedings of International Conference of Finite Elements in Nonlinear Solid and Structural Mechanics, Geiro, (Norway), (1977), 393
13) H. Ohtsubo, T. Hirakawa, and Y. Yamada: *Sosie to Kako (J. Jpn. Soc. Tech. Plasticity)*, **20**(1979)218, 235